Journal of Biomechanics ∎ (∎∎∎∎) ∎∎∎–∎∎∎

Contents lists available at ScienceDirect

Journal of Biomechanics

journal homepage: www.elsevier.com/locate/jbiomech
www.JBiomech.com

Spatial variations in Achilles tendon shear wave speed

Ryan J. DeWall [a,b,*], Laura C. Slane [c], Kenneth S. Lee [a], Darryl G. Thelen [c,d]

[a] Department of Radiology, University of Wisconsin-Madison, Madison, WI, USA
[b] Department of Medical Physics, University of Wisconsin-Madison, Madison, WI, USA
[c] Department of Biomedical Engineering, University of Wisconsin-Madison, Madison, WI, USA
[d] Department of Mechanical Engineering, University of Wisconsin-Madison, Madison, WI, USA

ARTICLE INFO

Article history:
Accepted 12 May 2014

Keywords:
Noninvasive mechanics
Shear wave imaging
Shear wave elastography
Tendon mechanics
Ultrasound elastography

ABSTRACT

Supersonic shear imaging (SSI) is an ultrasound imaging modality that can provide insight into tissue mechanics by measuring shear wave propagation speed, a property that depends on tissue elasticity. SSI has previously been used to characterize the increase in Achilles tendon shear wave speed that occurs with loading, an effect attributable to the strain-stiffening behavior of the tissue. However, little is known about how shear wave speed varies spatially, which is important, given the anatomical variation that occurs between the calcaneus insertion and the gastrocnemius musculotendon junction. The purpose of this study was to investigate spatial variations in shear wave speed along medial and lateral paths of the Achilles tendon for three different ankle postures: resting ankle angle (R, i.e. neutral), plantarflexed (P; R − 15°), and dorsiflexed (D; R+15°). We observed significant spatial and posture variations in tendon shear wave speed in ten healthy young adults. Shear wave speeds in the Achilles free tendon averaged 12 ± 1.2 m/s in a resting position, but decreased to 7.2 ± 1.8 m/s with passive plantarflexion. Distal tendon shear wave speeds often reached the maximum tracking limit (16.3 m/s) of the system when the ankle was in the passively dorsiflexed posture (+15° from R). At a fixed posture, shear wave speeds decreased significantly from the free tendon to the gastrocnemius musculotendon junction, with slightly higher speeds measured on the medial side than on the lateral side. Shear wave speeds were only weakly correlated with the thickness and depth of the tendon, suggesting that the distal-to-proximal variations may reflect greater compliance in the aponeurosis relative to the free tendon. The results highlight the importance of considering both limb posture and transducer positioning when using SSI for biomechanical and clinical assessments of the Achilles tendon.

1. Introduction

Achilles tendon injury, e.g. tendinopathy, can lead to chronic pain and impairment. The choice of treatment depends, in part, on the location and extent of injury. For example, conservative treatments such as eccentric exercises are more successful in treating mid-substance tendinopathy than in treating insertional tendinopathy at the calcaneus (Fahlstrom et al., 2003). However, identifying the location and severity of injury can be challenging, in part due to the complexity of Achilles tendon anatomy and mechanics. The Achilles tendon arises as the shared aponeurosis of the soleus, lateral gastrocnemius, and medial gastrocnemius (Wickiewicz et al., 1983), with each muscle exhibiting unique architectural features (Ward et al., 2009). The medial gastrocnemius has a larger physiological cross-section and more distal muscle–tendon junction than the lateral gastrocnemius (Ward et al., 2009; Wickiewicz et al., 1983), while the soleus inserts onto the Achilles tendon from the posterior side. Anatomical studies suggest that there is substantial inherent variability in these regional architectural features (O'Brien, 1984), which may factor into the location and presentation of tendon injury in an individual. Hence, there is a need for an improved understanding of the relationship between tendon anatomy and spatial mechanics, which could improve our ability to distinguish normal regional variations in tendon mechanics from those arising from tendon injury.

Ultrasound is often used to noninvasively elucidate tendon mechanics. For example, cine ultrasonic imaging can be used to track Achilles tendon motion and stretch with loading (Maganaris, 2003; Maganaris and Paul, 1999, 2002; Peixinho et al., 2008). Prior studies have identified spatial differences in tendon deformation, noting differences in stretch in the aponeurosis and the tendon for the same external load (Arampatzis et al., 2005; Arndt et al., 1998; Finni et al., 2003; Kubo et al., 1999; Maganaris and Paul, 1999; Magnusson et al., 2001, 2003; Muramatsu et al., 2001).

* Corresponding author at: Department of Radiology 1111 Highland Ave Madison, WI 53705, USA. Tel.: +1 616 405-9172.
E-mail address: ryandewall@gmail.com (R.J. DeWall).

http://dx.doi.org/10.1016/j.jbiomech.2014.05.008
0021-9290/

Additionally, imaging techniques broadly referred to as elastography have been applied to tendon biomechanics. Strain imaging, one form of ultrasound elastography capable of measuring high-resolution axial strain (Ophir et al., 1991), has been used to study tendon injuries. Tendon strain has been shown to be elevated in tendinopathic patients relative to healthy control subjects (De Zordo et al., 2010, 2009).

Ultrasound shear wave imaging techniques have emerged for mapping shear wave speeds within tissue (Bercoff et al., 2004; Nightingale et al., 2002; Sandrin et al., 2003). A technique called Supersonic Shear Imaging (SSI) generates shear waves using focused acoustic beams (i.e. acoustic radiation force) and then uses ultra-high frame rate ultrasonic imaging (Bercoff et al., 2004) to track these waves as they propagate. Shear wave speed can then be used as a non-invasive metric of tissue stiffness (D'Onofrio et al., 2010), because of its relationship to the shear modulus (Bercoff et al., 2004). SSI has previously demonstrated its ability to detect localized pathological changes in the stiffness of a variety of soft tissues, such as the breast, liver, and thyroid (Athanasiou et al., 2010; Bavu et al., 2011; Sebag et al., 2010). More recently, this method has been used to characterize activation- and length-dependent stiffness changes in muscle (Bouillard et al., 2011; Chernak et al., 2013; Gennisson et al., 2010; Koo et al., 2013; Maisetti et al., 2012; Nordez and Hug, 2010).

The application of SSI to tendon, however, has been studied less extensively. Shear wave speed in the free Achilles tendon has been measured (Arda et al., 2011; Aubry et al., 2013; Brum et al., 2014; Chen et al., 2013; Hug et al., 2013) and has been shown to increase as the tendon is stretched (Aubry et al., 2011, 2013). In the ruptured Achilles tendon, shear wave speed was significantly lower than in healthy tendons, and subsequently increased during the healing phase (Chen et al., 2013). In an *ex vivo* porcine partial tear model, regional shear wave speed was altered in the vicinity of tear damage (DeWall et al., 2014). SSI has also shown the onset of the rise in tension of the Achilles tendon with passive dorsiflexion (Hug et al., 2013). However, little is known about normal spatial variations in shear wave speed along the Achilles tendon.

Therefore, the purpose of this study was to investigate spatial variations in shear wave speed along medial and lateral paths of the Achilles tendon for three different ankle postures: resting ankle angle (R, i.e. neutral), plantarflexed (P; R – 15°), and dorsiflexed (D; R+15°). Prior work has shown greater stretch in the aponeurosis relative to the free tendon (Lieber et al., 1991; Maganaris and Paul, 2000), which may be a result of either intrinsic differences in tendon mechanical properties or changes in tendon cross sectional area. Based on this work, we hypothesized that the distal free Achilles tendon would exhibit greater shear wave speeds than its proximal aponeuroses.

2. Methods

2.1. Experimental protocol

Ten healthy young adults (aged: 26.7 ± 4.1 years, 5M/5F) with no history of tendon injury were recruited for this study. Prior to testing, written consent was obtained from each subject as per the Institutional Review Board requirements. The subject was then asked to walk at a comfortable pace for six minutes to precondition the muscle–tendon unit (Hawkins et al., 2009). Next, the subject was asked to lie prone on an examination table, with their foot extended and hanging off of the edge of the table. A standard clear plastic goniometer was used to measure the resting ankle angle (R, 26.3 ± 5.2° plantarflexion).

Ultrasonic B-mode images and shear wave data were collected using an Aixplorer clinical scanner (Supersonic Imagine; Aix-en-Provence, France; software version 5). All data were collected with the subject relaxed, and hence the plantarflexors in the passive state. The musculoskeletal preset was used with persist set to high and spatial smoothing set to 7. All data were collected by the same sonographer, with light transducer pressure applied. The left edge of a 50 mm linear array transducer (L15-4) was placed over the Achilles tendon distal insertion, and shear wave speed data were collected from five 10 mm × 10 mm boxes (the smallest size allowed) within the imaging field of view. The position of the proximal end of the transducer was then marked using a rubber band placed around the leg, and the transducer was moved proximally such that the distal edge of the transducer aligned with the rubber band, and the data collections were repeated. The transducer was moved proximally, i.e. in 50 mm proximal increments, until the collection location was at least 70 mm proximal of the gastrocnemius muscle–tendon junction. A custom 178 × 127 mm^2 ultrasound standoff pad (Aquaflex, Parker Laboratories, Fairfield, NJ) was used at the two most distal transducer positions. Trials were assigned a path along either the medial or lateral heads of the gastrocnemius (Fig. 1) for three postures: resting ankle angle (R), plantarflexed (P; R+15°), and dorsiflexed (D; R – 15°), in a random order.

2.2. Data analysis

Shear wave speed maps and maps of the quality of the shear wave speed estimates were stored in DICOM images exported from the system, and data were extracted using a research package script. A region-of-interest (ROI) was manually defined within the tendon for all images (Fig. 2) using a custom Matlab (Version 7.14) graphical user interface (GUI). The tendon was delineated from the muscle and surrounding tissue by looking for changes in echogenic intensity and echotexture on a given B-mode image in the region where shear wave speed was measured. Subsequently, the shear wave speed data were extracted from this ROI. From the ROI data, several parameters were computed, including the mean shear wave speed, ROI thickness, and ROI depth. ROI thickness was measured by finding the average number of pixels per column in the ROI and multiplying this number by the known distance per pixel (mm/pixel). ROI depth was measured by calculating the location of the center of mass of the ROI and measuring the distance to the skin surface. The spatial location of anatomical landmarks (calcaneus insertion (CI), soleus junction (SJ), and gastrocnemius aponeurosis (AP)) were measured from B-mode images (Fig. 2), with the CI defined as the start of the imaging path (0 mm). Because the locations of these landmarks vary (O'Brien, 1984), data were interpolated between them as follows: from the CI to SJ, the SJ to the AP (divided into three equally sized regions), and the AP+70 mm.

We also investigated the fidelity of the shear wave speed measurements using two metrics. First, we measured the quality of the shear wave speed estimates, which were also extracted from the user-defined ROI within the DICOM images using the research script. The quality metric is derived from the cross-correlation method used to estimate shear wave speed. Shear wave speed is estimated by tracking the shear wave using cross correlation, which compares the similarity of the shear wave shape at one time point to a later time point by convolving the two wave signals. The similarity of the waveforms is described by the correlation coefficient (values ranging from 0 to 1). Thus, a higher correlation coefficient would correspond with higher quality tracking and a higher fidelity shear wave speed estimate. Secondly, we calculated data saturation, which we calculated as the ratio of the pixels in the ROI at the maximum trackable shear wave speed of the system (16.3 m/s) divided by the total pixels.

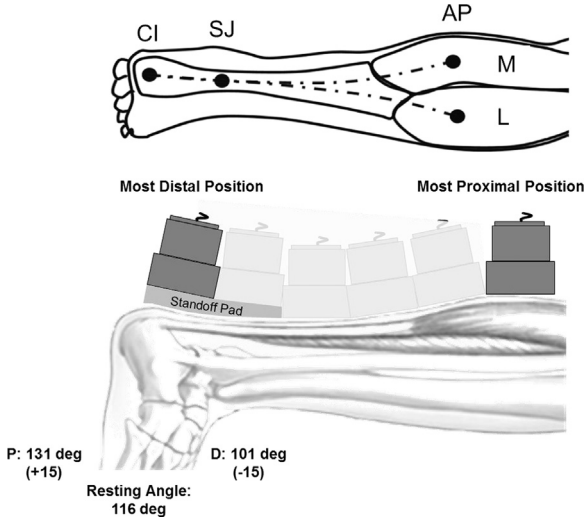

Fig. 1. Experimental methods. Shear wave speed was measured along two paths: medial (M) and lateral (L), for three different postures: plantarflexed (P), resting ankle angle (R), and dorsiflexed (D). Data were collected from an average of six transducer positions from the calcaneus insertion to 70 mm beyond the gastrocnemius muscle–tendon junction. Portions of this figure adapted from *Healthwise, Incorporated*.

Please cite this article as: DeWall, R.J., et al., Spatial variations in Achilles tendon shear wave speed. Journal of Biomechanics (2014), http://dx.doi.org/10.1016/j.jbiomech.2014.05.008